A study of the flexibility of the carbon catabolic pathways of extremophilic *P. aeruginosa* san ai exposed to benzoate *versus* glucose as sole carbon sources by multi omics analytical platform

Medić Ana, Nico Hüttmann, Marija Lješević, Yousef Risha, Maxim V. Berezovski, Zoran Minić, Ivanka Karadžić

PII: S0944-5013(22)00038-6

DOI: https://doi.org/10.1016/j.micres.2022.126998

Reference: MICRES126998

To appear in: *Microbiological Research*

Received date: 8 October 2021
Revised date: 17 February 2022
Accepted date: 26 February 2022

Please cite this article as: Medić Ana, Nico Hüttmann, Marija Lješević, Yousef Risha, Maxim V. Berezovski, Zoran Minić and Ivanka Karadžić, A study of the flexibility of the carbon catabolic pathways of extremophilic *P. aeruginosa* san ai exposed to benzoate *versus* glucose as sole carbon sources by multi omics analytical platform, *Microbiological Research,* (2021) doi:https://doi.org/10.1016/j.micres.2022.126998

A study of the flexibility of the carbon catabolic pathways of extremophilic *P. aeruginosa* san ai exposed to benzoate *versus* glucose as sole carbon sources by multi omics analytical platform

Medić Ana[a], Nico Hüttmann[b], Marija Lješević[c], Yousef Risha[b], Maxim V. Berezovski[b], Zoran Minić[b], Ivanka Karadžić[a,*]

[a] University of Belgrade, Faculty of Medicine, Department of Chemistry, Belgrade, Serbia [b] University of Ottawa, John L. Holmes Mass Spectrometry Facility, 10 Marie-Curie, Marion Hall, K1N 6N5, Ottawa, ON, Canada

[c] University of Belgrade, Institute of Chemistry, Technology and Metallurgy, Department of Chemistry, Njegoševa 12, 11000 Belgrade, Serbia

[*]Corresponding author

Ivanka Karadžić, E-mail: ivanka.karadzic@med.bg.ac.rs, Phone: +381113607067

Abstract

Polyextremophilic, hydrocarbonoclastic *Pseudomonas aeruginosa* san ai can survive under extreme environmental challenges in the presence of a variety of pollutants such as organic solvents and hydrocarbons, particularly aromatics, heavy metals, and high pH. To date, the metabolic plasticity of the extremophilic *P. aeruginosa,* has not been sufficiently studied in regard to the effect of changing carbon sources. Therefore, the present study explores the carbon metabolic pathways of polyextremophilic *P. aeruginosa* san ai grown on sodium benzoate *versus* glucose and its potential for aromatic degradation. *P. aeruginosa* san ai removed/metabolised nearly 430 mg/L of benzoate for 48 hours, demonstrating a high a capacity for aromatic degradation. Comparative functional proteomics, targeted metabolomics and genomics analytical approaches were employed to study the carbon metabolism of the *P. aeruginosa* san ai. Functional proteomic study of selected enzymes participating in the β-ketoadipate and the Entner-Doudoroff pathways revealed a metabolic reconfiguration induced by benzoate compared to glucose. Metabolome analysis implied the existence of both catechol and protocatechuate branches of the β-ketoadipate pathway. Enzymatic study of benzoate grown cultures confirmed the activity of the *ortho*- catechol branch of the β-ketoadipate pathway. Even high concentrations of benzoate did not show increased stress protein synthesis, testifying to its extremophilic nature capable of surviving in harsh

conditions. This ability of *Pseudomonas aeruginosa* san ai to efficiently degrade benzoate can provide a wide range of use of this strain in environmental and agricultural application.

Keywords:

Pseudomonas aeruginosa; carbon metabolism; benzoate; proteome; metabolomics; biodegradation

1. Introduction

Plasticity of metabolic pathways of *Pseudomonas aeruginosa*, in particular central and peripheral carbon metabolism, seems to be one of the adaptive strategies employed to survive harsh environmental conditions (Berger et al., 2014). These unique genetic and metabolic characteristics such as versatility of carbon metabolism of *Pseudomonas*, especially environmental isolates, confirm its potential for application in fields of biotechnology and bioremediation of polluted sites, including agricultural environment (Cao et al., 2008; Tsirogianni et al., 2004; Xiang et al., 2020; Yun et al., 2011;).

Many aromatic compounds are considered to be environmental pollutants that can adversely affect flora and fauna, resulting in the entry of toxic compounds into the food chain causing serious health problems and genetic damage to humans. Due to their toxicity, mutagenicity and carcinogenicity, the Environmental Protection Agency classifies aromatic compounds as priority pollutants (Benedek et al., 2020). Benzoic acid (E210) and its salt sodium benzoate (E211) have been used as preservatives for foods and cosmetics. They are considered to possess low acute oral and dermal toxicity (EU, SCCP/0891/05), with the maximal allowed amount of 150- to 500 mg/kg in foodstuffs.

Benzoic acid naturally occurs in some plants, with particularly high concentration of 0.05%- 0.13% in berries. On the other hand, benzoic acid is an allelochemical found in root exudates and rhizosphere soil of crops having a detrimental effect on other species and causing problems associated with crop replanting. The bioremediation of allelochemicals by microorganisms has been considered as an efficient degradation process (Xiang et al., 2020). In particular, the genus *Pseudomonas* with its great metabolic versatility can metabolize diverse aromatic compounds including ones derived from plants or from the decomposition of plant material.

Fourteen different pathways of aromatic catabolism in *Pseudomonas* have been confirmed and under specific growing condition multiple pathways can be utilize (Nogales et al., 2017). Benzoate is often used as a model compound to investigate the possibility of microbial degradation of aromatic compounds because it is the simplest known aromatic intermediate in the biodegradation of various complex polyaromatic compounds. The obtained information on the bacterial degradation of benzoate can be further used to understand and predict the degradation pathways of more complex aromatic compounds. A major pathway for the catabolism of aromatic compounds in bacteria is the β- ketoadipate (KA) pathway, wherein aromatic compounds are transformed into non-toxic metabolites. Through the action of mono- and dioxygenases, the resonant structure of aromatic compounds is destabilized and ring cleavage occurs, producing intermediates such as catechol or protocatechuate, whose catabolites are further used in the tricarboxylic acid cycle (Ghosal et al., 2016; Varjani et al., 2017).

A good knowledge of the metabolic pathways in microorganisms enables new strategies for the treatment of a broad range of pollutants in the environment, including agricultural surroundings. Comprehensive analyses using newly developed methods from genomics, proteomics, and metabolomics would greatly improve the understanding of all processes that take place during the microbial decomposition of pollutants (Chauhan and Jain, 2010; Weimer et al., 2020). Analytical omic methods enable the study of early molecular responses of the organism to sources of pollution and as such can be used to identify a specific metabolic response to a toxic substance, detect new biomarkers and predict the effects of pollutants on organisms and the environment (Gouveia et al., 2019).

Although the carbon metabolism pathway of *P. aeruginosa* appears to be fully elucidated, it is extrapolated from known metabolism pathways of other species of the genus *Pseudomonas*. In fact, carbon metabolism in *P. aeruginosa* exposed to different carbon sources in different environments has not been sufficiently studied so far (Dolan et al., 2020). In addition, the metabolism of extremophilic *P. aeruginosa*, which has the potential to degrade organic contaminants, is particularly unexplored in terms of not only the diversity of carbon metabolic pathways but also changes in numerous other metabolic functions.

P. aeruginosa san ai is an environmental isolate with a great potential for use in biotechnology (Karadzic et al., 2004; Karadžić et al., 2006; Rikalović et al., 2013), and

bioremediation of heavy metals (Avramović et al., 2013; Izrael-Živković et al., 2018) and organic chemical pollutants (Medić et al., 2019; 2020). This is the first comprehensive study of benzoate degradation by polyextremophilic *Pseudomonas aeruginosa* at the level of the targeted metabolomic analysis of products of benzoate degradation and related enzymatic activity, and comparative functional proteomics analysis of cultures grown on benzoate and glucose to reveal affected biochemical pathways. Glucose and benzoate are selected as substrates of similar preferability for *P. aeruginosa*, providing comparable growth conditions, as glucose is assimilated through central metabolic pathways, and benzoate is degraded *via* peripheral catabolic pathways.

2. Material and methods

2.1.Bacterial strain and culture conditions

The microorganisms used for sodium-benzoate (NaB) degradation was *Pseudomonas aeruginosa* san ai, an environmental isolate from mineral cutting oil (Karadzic et al., 2004). The strain is deposited as NCAIM B.001380 in National Collection of Agricultural and Industrial Microorganisms (NCAIM), Corvinus University of Budapest, Budapest, Hungary, and in the public collection of bacteria WDCM 375 (Institute of Soil Science, Department of Soil Microbiology, Belgrade, Serbia), with accession number ISS 619.

P. aeruginosa san ai was activated on nutrient agar (Torlak, Belgrade, Serbia) at 30 ºC for 24 h and used for inoculation. To examine influence of benzoate on *P. aeruginosa* san ai minimal salt medium (MSM) was supplemented with increasing concentrations of NaB 0.2- 2 g/L and optical density as a measure of growth was monitored during 5 days. Experiments of NaB degradation, metabolome, and proteome study were conducted in 500 mL Erlenmeyer flask, containing 100 mL of minimal salt medium (MSM) supplemented with 3 mM NaB as a sole carbon and energy source, while glucose (5 mM) was used as a control substrate. Inoculation was performed so that the initial colony-forming unit (CFU) value was approximately $4x10^7$. The MSM was prepared as described previously (Medić et al., 2020).

All batch cultures were incubated at 30 ºC on a horizontal shaker (Kuhner, Basel, Switzerland) at 150 rpm for 7 days. Control of non-biological degradation containing MSM medium supplemented with NaB and glucose without inoculums were carried out. All experiments were performed in three replicates.

Bacterial growth was monitored spectrophotometrically using a Shimadzu model UV-2600 spectrophotometer (Shimadzu Kyoto, Japan). Absorbance was measured against sterile non-inoculated mineral medium at a wavelength of 580 nm (Heyd et al., 2008). Bacterial concentration was estimated to be $3x10^8$ cells/mL which corresponded to absorbance of 0.47 at 580 nm.

2.2.Effects of sodium benzoate on growth of P. aeruginosa san ai

Effects of increasing NaB concentrations, ranging from 0.2-22 mg/mL, on the growth of *P. aeruginosa* san ai in Lurie Bertani (LB) medium was assessed using the tube dilution method (NCCLS, 1997). Tubes containing growth medium and increasing concentrations of NaB were inoculated with suspension of 24 h old culture of *P.aeruginosa* san ai, previously grown on nutrient agair, to obtain an initial optical density of 0.05, at 580 nm. Microbial growth was measured turbidimetrically during 26 h using Clormic (Selecta, Spain). The minimal inhibitory concentration was defined as the lowest concentration of NaB at which there was no visible growth of the microbe after 24 h. Experiments were performed in three replicates.

2.3.Respiration analysis

Culture growth and development on NaB and glucose as C sources, were monitored as respiration rates of cumulative oxygen consumed and carbon dioxide produced (mL). The analysis of the respiration of *P. aeruginosa* san ai was run on Micro Oxymax respirometer (Columbus Instruments, Columbus, USA). The experiments were performed in Micro Oxymax light- proof 500 mL bottles (Duran, Wertheim, Germany) containing 100 mL of MSM supplemented with 3 mM NaB and 5 mM glucose and stirred constantly (150 rpm) with magnetic stirrer (Heidolph, Schwabach, Germany) at 25 ºC for seven days. A sterile medium with NaB or glucose were used as non- biological controls, while inoculated MSM without NaB or glucose were used as biological controls. Cell respiration was measured every 240 min for seven days. All experiments were performed in three replicates. Obtained data were evaluated by Micro Oxymax software.

2.4.Enzyme assays

The activities of hydroxylase, catechol 1,2-dioxygenase (C12O) and catechol 2,3-dioxygenase (C23O) were performed spectrophotometrically using a UV-2600 (Shimadzu,

Kyoto, Japan) UV/VIS spectrophotometer by measuring the absorbance at 340, 260 and 375 nm, respectively, as previously described (Medić et al., 2019; 2020).

2.5.Comprehensive two-dimensional gas chromatography-mass spectrometry analyses of substrate and metabolites during benzoate degradation

To determine NaB metabolites, after 11 h, 24 h, 48 h and 7 days of incubation, each whole flask culture was first acidified to pH 2.5 with 0.1 M HCl then extracted three times with ethyl acetate. The extracts were dried with anhydrous Na_2SO_4, concentrated by rotary evaporation to a constant weight. The solid residue was dissolved in 100 µL ethyl acetate then derivatized using 100 µL of BSTFA + TMCS (Sigma-Aldrich) for 40 min at 60 °C.

Derivatized samples were analyzed using a Shimadzu's comprehensive GC x GC-MS system, comprising of GC-MS-QP2010 Ultra with a ZX2 thermal modulation system (Zoex Corp.). The system and method used for the analysis were reported in our previous study (Medic et al, 2020). The first dimension column was a RtxR-1 (RESTEK, CrossbondR 100% dimethylpolysiloxane, 30 m x 0.25 mm, 0.25 µm) and the second one was a BPX50 (SGE Analytical Science, 1 m x 0.1 mm, 0.1 µm). The following temperature program was used: 40 °C for 5 min, then 5 °C/ min to the final temperature 300 °C (5 min). The modulation period was 6 s. The collected mass range was m/z of 70 to 500. The data were analyzed using GCImage R2.8 (GCImage LLC), and metabolites were identified tentatively by comparison to the NIST library in order to narrow down the list of potential metabolites, then compared manually to the library and published literature (Katayama-Hirayama et al., 1991a; Katayama-Hirayama et al., 1991b) to confirm identification. Degradation percentage was estimated using the volume of each blob in the GC x GC-MS chromatograms.

2.6.Comparative proteomic analysis

2.6.1. Sample preparation

Biomass of cells grown in MSM medium supplemented with different C-sources (NaB and glucose), in the early stationary phase were collected by centrifugation at 10000 rpm for 20 min. using Sorvall with SS-1 rotor (United Kingdom), washed two times by 50 mM Tris buffer, pH 7.5 supplemented with 0.1 mM phenylmethylsulfonyl fluoride (PMSF) and 0.5 mM 1,4-dithiothreitol (DTT), and frozen. Biomass was homogenized in two volumes of the same buffer at 4 °C, using a glass Teflon homogenizer, and ultracentrifuged for 2 h at 100

000g at 4 °C using BeckmanCoulter L5-65 with SW 28 rotor (Beckman, Indianapolis, USA). The protein extracts in the supernatants were used for proteomics study and enzyme assays. Protein content was determined by Bradford`s assay (Bradford, 1976).

2.6.2. Protein reduction, alkylation and in solution enzymatic digestion

Samples were reduced with 3 mM TCEP for 45 min at room temperature then alkylated with 15 mM iodoacetamide for 60 min in the dark at room temperature. Proteolytic digestion was performed by addition of Trypsin/Lys-C solution, 500 ng (Promega, V5072, Madison, USA) and incubated under shaking at 500 rpm at ambient temperature overnight. The digestion was stopped by addition of formic acid (1% final concentration) and centrifuged at 15,000 x g for 2 minutes. The supernatant containing about 50 µg of digested protein was desalted on disposable TopTip C-18 columns (Glygen, # TT2C18.96, Maryland, USA) and dried by vacuum centrifugation.

2.6.3. *LC-MS/MS*

Orbitrap Fusion (Thermo Scientific, Massachusetts, USA) coupled to an Ultimate3000 nanoRLSC (Dionex, California, USA), was used for LC-MS/MS analysis of digested proteins. A detailed description of interment settings is provided in our previous work (Risha et al., 2020). An in-house packed column (polymicro technology), 15 cm x 70 µm ID, Luna C18(2), 3 µm, 100 Å (Phenomenex, California, USA) was used for peptides separation by a water/acetonitrile/0.1% formic acid gradient. Samples were loaded onto the column for 200 min at a flow rate of 0.30 µL/min. Peptides were separated using 2% acetonitrile in the first 7 min and then using a linear gradient from 2 to 35% of acetonitrile for 133 min, followed by gradient from 35 to 98% of acetonitrile for 20 min, then at 98% of acetonitrile for 15 min, followed by gradient from 98 to 2% of acetonitrile for 10 min and wash 15 min at 2 % of acetonitrile. Eluted peptides were directly sprayed into mass spectrometer using positive electrospray ionization (ESI) at an ion source temperature of 250 °C and an ionspray voltage of 2.1 kV. The Orbitrap Fusion Tribrid was programmed in the data dependent acquisition mode. MS spectra (m/z 350–2000) were acquired at a resolution of 60 000. Peptide precursor ions were filtered according to monoisotopic precursor selection, charge state (+2 to +7), and dynamic exclusion (70 s with a ± 10 ppm window). The automatic gain control settings were 5e5 for full FTMS scans and 1e4 for MS/MS scans. Collision-induced dissociation (CID) in

the linear ion trap was used for fragmentation. Precursors isolated using a 2 m/z isolation window were fragmented with a normalized collision energy of 35%.

2.6.4. MS Data Analysis

MS raw files were analyzed with MaxQuant, version 2.0.1.0 (Cox and Mann, 2008) and the Andromeda search engine (Cox et al., 2011). Peptides were searched against the reference genome for *Pseudomonas aeruginosa* PA01 (NCBI taxonomy Id: 208964; 5564 entries) and a contaminants database. Default parameters were used if not mentioned otherwise. Modifications were set as following: N-terminal acetylation and methionine oxidation as variable modifications, and cysteine carbamidomethylation as a fixed modification. Six amino acids as minimum peptide length, and false discovery rate (FDR) of 0.01 for both the protein and peptide level, determined by searching against a reverse decoy database, were set. A maximum of two missed cleavages was set. Peptides were identified with an initial precursor mass deviation of up to 10 ppm and a fragment mass deviation of 0.5 Da. The 'Match between runs' algorithm in MaxQuant (Nagaraj et al., 2012) was performed between all samples to increase peptide identification rate. Proteins matching to the reverse database or only identified by modified peptides were discarded.

Peptide counts and label-free quantification (LFQ) intensity from the MaxQuant *proteinGroups* output file were used for analysis of differential protein abundance under different conditions. Valid LFQ intensities were required in at least 50% of samples to compute log2 fold-change and p-value by unpaired t-test for proteins. Missing values were imputed based on a shifted normal distribution (shift = 1.8 standard deviations (sd), width = 0.3 sd).

2.7.Genome and metabolic pathways analysis

P. aeruginosa san ai genome and metabolic pathways were analyzed by the databases IMG (Integrated Microbial Genomes), https://img.jgi.doe.gov/cgi-bin/m/main.cgi, (Chen et al., 2019) and KEGG (Kyoto Encyclopedia of Genes and Genomes), https://www.genome.jp/kegg/ (Kanehisa et al., 2020).

3. Results and Discussion

3.1.Effects of sodium-benzoate on growth of the P. aeruginosa san ai

The growth of *P. aeruginosa* san ai, in complex medium, in the presence of increasing NaB concentrations (0.2 - 22 mg/mL) and control (no added NaB) is shown in Fig. 1a. Compared to control, a low concentration of 0.2 mg/mL NaB caused no measurable change in microbial growth after 24 h, while increasing the concentration to 0.5 mg/mL led to a slight increase in microbial growth of approximately 4.4%. When exposed to NaB concentrations of 1, 2, 4, and 9.0 mg/mL, the growth of *P. aeruginosa* san ai was inhibited by 3.0 (data not shown), 7.3, 11.3, and 28.7%, respectively (Fig. 1a). NaB concentration of 0.5 mg/mL, which caused a small increase in biomass, was taken as optimal, whereas higher concentrations were considered inhibitory since they caused a metabolic redirection so that there was no further increase in biomass. A marked decrease in growth associated with strongest inhibition was observed at a concentration of 18 mg/mL which is considered as the minimal inhibitory concentration (MIC) of benzoate. A MIC of sodium benzoate against *P. aeruginosa* san ai of 18 mg/mL, obtained in this study, is significantly higher than the reported MIC of 5 mg/ml against *Pseudomonas aeruginosa* (Stanojevic et al., 2009). Our results clearly show high resistance, so that even in the presence of NaB concentrations as high as 9 mg/mL, in complete medium, the growth of *P. aeruginosa* san ai was only reduced by less than 29% (Fig. 1a).

3.2.Efficiency of biodegradation of sodium-benzoate by P. aeruginosa san ai

Within the range of benzoate concentrations of 0.2 to 2 mg/mL, in MSM, *P. aeruginosa* san ai grew well with a slightly reduced biomass yield of less than 10% for concentrations above 1 mg/mL, implying the potential use of benzoate as the sole carbon and energy source. The concentrations of NaB in the environment is far lower than the determined MIC of NaB against *P. aeruginosa* san ai. Amount of benzoic acid and sodium benzoate into water and soil as a result of anthropogenic activities were estimated to be less than 20 mg/kg (CICAD, 2005), while in case of alleopathy, where benzoic acid and its derivatives were considered to be the predominant cause of crop autotoxicity, their concentrations are a bit higher, up to 0.5 mmol/L (0.072 mg/mL) (Hunag et al., 2020; Xinag et al., 2020). Taking these concentrations into account, as well as the optimum growth of *P. aeruginosa* san ai determined on the complex medium, the growth of *P. aeruginosa* san ai in MSM supplemented with 3 mM NaB (0.432 mg/mL) was examined and shown in Fig. 1b. As is depicted, the CFU/mL values were increased exponentially during the first 48 h of incubation implying an intense growth of *P. aeruginosa* san ai that confirms that *P. aeruginosa* san ai

can survive and successfully use NaB as the sole source of carbon and energy. As shown in Fig. 1c, NaB disappeared from the MSM growth medium within 48 h implying its efficient biodegradation by *P. aeruginosa* san ai. The results of the GCx GC-MS analysis showed that nearly 99% NaB was removed from the total amount of 0.432 mg/mL within 48 h. The decrease in NaB was associated with an increase of cell density.

Several other species of *Pseudomonas* were reported to degrade benzoate with varying degradation abilities. *Pseudomonas* sp. QTF5 degraded 12.4% benzoate at a concentration of 3 mg/mL over 3 days (Li et al., 2017). *Pseudomonas* sp. SCB32 degraded more than 97% of benzoic acid (0.800 mg/mL) in 24 h (Xiang et al., 2020). *P. putida* ATCC 49451 completely degraded 0.400 mg/mL of benzoate in 12 h (Loh et al., 2002), while at the same time the WH-B3 strain degraded more than 90% of benzoate at an initial concentration of 0.500 mg/mL (He et al., 2019). With a degradation rate of 0.427 mg/mL in 48 h, *P. aeruginosa* san ai represents a microorganism with a high biodegradation capability. Furthermore, the tolerable value of 0.400 mg/mL, is far higher than the concentrations of benzoic acid in the environment indicating that *P. aeruginosa* san ai has a great application potential.

3.3.Respiratory activities of P. aeruginosa san ai

Pseudomonas is able to assimilate a wide range of compounds as a source of carbon and energy, which allows it to survive and adapt to a broad range of environmental conditions. The preferred carbon sources for *Pseudomonas* are organic compounds, particularly succinic acid, followed by a few amino acids then glucose, while hydrocarbons are the least preferred compounds (Rojo, 2010). Furthermore, in complete medium induction of the genes responsible for degradation of some hydrocarbons is inhibited as a result of carbon catabolite repression that allow cells to selectively assimilate a preferred compound from a mixture of several potential carbon sources (Rojo, 2010). To avoid a repressing effect on the expression of genes responsible for metabolism of a certain carbon source, minimal salt medium (MSM) was used and effect of two less preferable C sources/ compounds- NaB and glucose on growth was examined.

To confirm and monitor the growth of *P. aeruginosa* san ai on selected sole carbon sources- NaB and glucose - the respiratory activity was analyzed and compared by measuring the cumulative oxygen consumed and carbon dioxide produced (Fig 1. c and d). The most intensive respiration occurred in the first 40 h, with cumulative O_2 consumption of 45 mL for

NaB and 49 mL for Glc and cumulative CO_2 production of 36 mL (NaB) and 48 mL (Glc). The similarity in growth rate when cells used glucose or NaB, as the sole C- source, implies that the two compounds are equally good carbon sources. Besides, it is worth mentioning that of the expected 3.3 mmol and 2.5 mmol of CO_2 produced as a result of metabolism of glucose and NaB metabolism, respectively, only 65% was detected. Since CO_2 is the final metabolism product of both C-sources, it can be inferred that two-thirds of the available carbon sources were completely degraded and consumed in respiratory metabolism while the remaining third of carbon content was used for anabolism and growth. As starting amounts of glucose and NaB were in the ratio of 1.85 : 1, detected differences in growth efficacy were expected (Fig. 1b). The degradation percentage of 98.8% obtained by the GC x GC-MS analysis of NaB, suggests that the C source was completely exhausted. From a bioremediation point of view, these results clearly show promising potential for the aerobic biodegradation of NaB by *P. aeruginosa* san ai.

Fig. 1.

3.4.Versatility of catabolic carbon pathways in P. aeruginosa san ai

Physiological studies of catabolic pathways undoubtedly showed that bacterial growth at the expense of a single substrate promotes cells with the ability to oxidize the specific substrate and its catabolites. In response to varying carbon sources, certain catabolic pathways are inducible in *Pseudomonas* (Ornston,1971). Compared to other Gram-negative bacteria, *Pseudomonas* transported and metabolized glucose in a specific way *via* the Entner-Doudoroff (ED) pathway instead of the more common Embden-Meyerhof-Parnas (EMP) glycolytic pathway (del Castillo et al., 2007). Accordingly, induction of enzymes of the ED pathway (glucose-6-phosphate 1-dehydrogenase, 6-phosphogluconolactonase, phosphogluconate dehydratase, and 2-keto-3-deoxy-phosphogluconate aldolase) in *P. aeruginosa* san ai grown on glucose was anticipated. Indeed, *P. aeruginosa* san ai catabolizes glucose only through the ED pathway to subsequent glycolytic steps and further to pyruvate as shown in Fig. 2. The ED pathway and the TCA cycle are found to be exclusive catabolic pathways of glucose catabolism in *P. aeruginosa* san ai. All enzymes of the ED and the TCA cycle in *P. aeruginosa* san ai are upregulated (Fig. 2). Unlike other bacteria which use a soluble NADH-producing malate dehydrogenase, *P. aeruginosa* converts malate to oxaloacetate by malate-quinone dehydrogenase (MQO) (Dolan et al., 2020, Gorisch et al.,

2002). Using fluxomic analysis, it was recently demonstrated that more than two-thirds of the carbon from malate was converted to pyruvate by malic enzymes, trough the pyruvate shunt, while less than a third was transformed to oxaloacetate by malate dehydrogenase (Dolan et al., 2020) (Fig. 2).

The pseudomonads can metabolize structurally diverse aromatic molecules into a few central aromatic intermediates through peripheral catabolic pathways considered as 'metabolic funnels.' Although, the β-ketoadipate pathway is one of the most prevalent metabolic funnels induced by benzoate, it should be noted that the ability to degrade aromatic compounds is strain-specific and that several pathways can be present in some strains but absent in others even within the same species (Nogales et al., 2017). As the induction of the KA by benzoate in *Pseudomonas aeruginosa* has not been studied to date, so the current investigation addresses the gap, and provides insight into the metabolism of a polyextremophilic, hydrocarbonoclastic bacterium of this species.

The study of the ED and benzoate metabolic pathways based on *P. aeruginosa* san ai genome annotations showed existence of all the genes coding for enzymes involved in the ED and the KA pathways of the catechol and protocatechuate branches (Table 2, 3), as previously reported (Medić et al., 2019). To fully explore benzoate catabolic pathways in *P. aeruginosa* san ai, metabolomic and enzymatic analyses were applied, in addition to a functional proteomic analysis of NaB- and glucose- grown cells.

3.5.Targeted metabolome study

To confirm the genomic prediction, the metabolites of benzoate degradation were analyzed using a GC-GCxMS approach and identified as shown in Fig. 2.

Fig. 2.

As shown in Fig. 1c *P. aeruginosa* san ai degraded benzoate very quickly, so metabolites generated after 24 h were analyzed and the mass spectrum and retention time of compounds clearly confirmed the presence of seven benzoate metabolites (Fig. 3, Table 1.) such as: 3,4-dixydroxybenzoate, catechol, *cis, cis*-muconic acid, muconolactone, β-ketoadipate enol-lactone and succinic acid as the end products of the benzoate transformation

(Fig. 2). The detected benzoate metabolites indicate the degradation of NaB through the catechol branch of β-ketoadipate degradation pathway, followed by the *ortho*- cleavage of catechol. Furthermore, the identified protocatechuate implicates the second branch of the KA pathway. In sterile MSM without inoculation, no target metabolites of benzoate degradation were detected throughout the experiment. Taken together, our results implicate both branches of the KA pathway in the degradation of benzoate.

Fig. 3.

Table 1 GCxGC retention times and mass spectral data of benzoate and its metabolites detected in this study.

Compound number referred to in Fig. 3	Retention time (min)	*m/z* (% of relative intensity)	Metabolite identification
I	25.70	179 (100), 105 (67), 135 (50), 77 (44)	Benzoic acid trimethylsilyl ester
II	28.20	73 (100), 239 (16), 72 (15), 74 (13), 254 (12)	1,2-Benzenediol bis(trimethylsilyl) ether (Catechol, 2TMS)
III	34.40	169 (100), 73 (82), 147 (62), 170 (19, 168 (17), 271 (13)	2-Furanacetic acid, α-[(trimethylsilyl)oxy]-, trimethylsilyl ester (*cis, cis*- Muconate, 2TMS)
IV	30.80	75 (100), 73 (89), 157 (76), 199 (51), 81 (48), 155 (43), 111 (41), 85 (40)	Cyclohexanone-3-carboxylic acid, trimethylsilyl ester (Muconolactone, TMS)
V	35.09	73 (100), 147 (75), 77 (46), 271 (51), 75 (33)	2,4-Hexadienedioic acid, bis(trimethylsilyl) ester, (E,E) (β- ketoadipate enol lactone, 2TMS)
VI	27.80	147 (100), 73 (87), 148 (22), 75 (21), 291 (14),	Butanedioic acid, bis(trimethylsilyl) ester

		74 (14), 146 (13), 72 (13), 247 (12)	(Succinic acid, 2TMS)
VII	40.60	73 (100), 193 (70) 72 (19) 75 (18), 194 (15), 370 (15), 147 (14), 74 (13), 355 (11)	Benzoic acid, 3,4-bis[(trimethylsilyl)oxy]-, trimethylsilyl ester (Protocatechuate, 3TMS)

Some intermediate metabolites, such as 1,2-dihydro-1,2-dihydroxybenzoic acid, were not detected due to their rapid consumption or unstable and quick transformation (Chae and Yoo, 1997; Xiang et al., 2020). The catechol, *cis, cis*- muconat, oxoadipate and succinate metabolites identified in this study are in agreement with the *ortho*-cleavage of benzoate by *P. putida* F1 (Mandalakis et al., 2013), and benzoic acid by *Pseudomonas sp.* SCB32 (Xiang et al., 2020).

3.6.Proteome study

Numerous authors demonstrated the usefulness of proteomic analysis for predicting and understanding bacterial metabolic pathways of aromatic compounds degradation (Cao and Loh, 2008; Tsirogianni et al., 2004; Vandera et al., 2015). Using a proteomic analysis, Yun et al. (2011) confirmed the expression of benzoate degradation enzymes with putative metabolic pathway enzymes in *Pseudomonas putida* KT2440. Moreover, the catechol 1,2–dioxygenase pathway was identified as the major pathway induced by benzoate exposure in *Pseudomonas* sp. K82 and *Pseudomonas putida* KT 2440 (Kim et al., 2004; 2006). However, to date benzoate assimilation by *Pseudomonas aeruginosa* has not been monitored by proteomic analytical platforms. Even more, benzoate degradation by polyextremophilic, hydrocarbonoclastic pseudomonades, such as *P. aeruginosa* san ai has not yet been studied.

Taking into account that cells grown in a minimal salt medium containing the aromatic substrates as the carbon source have potential for strong and immediate pathway induction (Hugouvieux-Cotte-Pattat et al., 1990), we compared by functional proteomics the effects of NaB and glucose, as equally preferred substrates, on the metabolism of *P. aeruginosa* san ai grown in MSM. Tryptic peptide mixtures were analyzed by an Orbitrap Fusion mass spectrometer for protein identification. In total, 11753 peptides were assigned to 1394 proteins which represent 25% of the total *P. aeruginosa* san ai proteome: 1094 common,

108 unique to glucose, 192 unique to NaB, identified in at least 2/3 replicates (Fig. 4). Compared to the other published works, this study provides a deeper profiling of the *P. aeruginosa* proteome. Using iTRAQ-labeling and LTQ mass spectrometer, a total of 570 proteins were identified and 107 were differentially expressed in *P. putida* KT2440 grown in benzoate *versus* succinate (Yun et al., 2011). In addition, Tandem Mass Tag (TMT) isobaric labeling of peptides with 2D LC-ESI-MS/MS on an LTQ Orbitrap XL mass spectrometer, proteomic analysis of *P. putida* F1 resulted in identification of 1900 proteins, with 46 proteins upregulated in citrate-grown cells, five of which were exclusively identified, while 53 proteins were upregulated in the benzoate-grown cells and three of the proteins being found uniquely (Mandalakis et al., 2013).

In the present study peptide counts and label-free quantification (LFQ) intensity from the MaxQuant *proteinGroups* output file were used for analysis of protein expression under different conditions. Comparison of peptide counts clearly shows the presence and absence of certain proteins under different condition. Under NaB- growth conditions a number of 11 unique proteins belonging the benzoate degradation pathway were found. Glucose amended cultures uniquely identified proteins related to ED pathway activation.

COG functional analysis revealed unique category Q of the secondary metabolism that refers to aromatic compounds metabolism in benzoate amended culture, while in glucose grown culture proteins responsible for extracellular structures synthesis (W) were found to be uniquely expressed (Fig. 4b, c). COG functional classification of uniquely identified proteins from *P. aeruginosa* san ai also indicates pronounced lipid (I category) metabolism, secretion (U category) and defense (V category) in benzoate- grown culture, whereas enhanced energy production (C category), transcription (K category) and posttranslational modifications (O category) were enhanced in glucose amended culture. Although most the of identified proteins belong to both cultures, analysis of unique proteins indicates complex control of metabolic networks which is triggered by the utilization of the different carbon sources.

Fig. 4.

For functional proteome analysis, pathway annotations were obtained from the KEGG database. Three key pathways: benzoate degradation, (KEGG-Id: pae00362), glycolysis / gluconeogenesis (KEGG-Id: pae00010) and citrate cycle/ TCA cycle (KEGG-Id: pae00020) were identified by 22/36, 28/33, 27/28, respectively; while Entner-Doudoroff pathway

(KEGG-Id: 0030) was identified with all of its 4 participating proteins. These results revealed significant metabolic reconfiguration at the proteome level between glucose- and NaB- grown cultures.

3.6.1. Preferentially expressed proteins

3.6.1.1.Enzymes of the Entner-Doudoroff pathway

All enzymes of the ED pathway- glucose-6-phosphate 1-dehydrogenase, 6-phosphogluconolactonase, phosphogluconate dehydratase, and 2-keto-3-deoxy-phosphogluconate (KDPG) aldolase - were identified to be up regulated only in glucose grown cultures (Table 2, Fig. 2), supporting the inducible nature of the ED.

Aside from the ED pathway, in glucose-grown culture energy production is pronounced, with enhanced biosynthesis of FAD- and NADH- dependent dehydrogenases or oxidoreductases, (Fig. 4, Table S1). With energy related, proteins responsible for motility are also up-regulated in glucose- grown culture (Fig. 4b, c), accordingly to (Mandalakis et al., 2013) and (Domínguez-Cuevas et al., 2006) who suggested that the repression of motility caused by benzoate may serve as an adaptive bacterial response to save energy (Table S2). Furthermore, the negative regulators of the sigma factor AlgU which plays a role in the differentiation of *P. aeruginosa*, triggering the synthesis of exopolysaccharide alginate, is up regulated in glucose amended culture (Fig. 4b, c, Table S2).

Table 2 Enzymes of the Entner-Doudoroff pathway, during the growth of *P. aeruginosa* san ai on sodium-benzoate and glucose. Number of identified peptides per protein from 3 biological replicates is shown. List of enzymes is based on KEGG-Id: 0030.

Accession	Protein name	Gene	Peptides Glc	Peptides NaB
O68282	Glucose-6-phosphate 1-dehydrogenase	zwf	7/7/7	1/0/0
Q9X2N2	6-phosphogluconolactonase	pgl	3/2/2	1/0/0
P31961	Phosphogluconate dehydratase	edd	8/7/9	0/1/1

O68283	2-keto-3-deoxy-phosphogluconate aldolase	eda	2/2/1	0/0/0

3.6.1.2.Enzymes of the benzoate biodegradation pathway

Out of the 192 differentially expressed proteins found in benzoate grown cultures, 19 proteins were identified from eight steps of benzoate degradation *via* the catechol and protocatehuate *ortho*-cleavage pathways (Fig. 2), starting from the initial oxidation of benzoate to final formation of succinyl-CoA intermediate of the TCA cycle (Table 3), (Harwood and Parales, 1996). The complete list of proteins involved in benzoate degradation *via* the catechol *ortho*-cleavage pathway, and two of four proteins from the protocatehuate pathway were found uniquely in NaB grown culture. The catechol branch comprises of: toluate 1,2-dioxygenase (Q9I0W4, Q9I0W5) and 1,2-dixydroxycyclo hexa-3,4-diene-1-carboxylate dehydrogenase (Q9I0W7), which initiate the process of benzoate transformation by oxidation to 1,2 -dihydroxy derivatives. This is followed by catechol 1,2-dioxygenase (Q9I0X5) which converts dihydroxy derivative to catechol, further transformed by muconate cyclo-isomerase (Q9I0X3) and muconolactone delta-isomerase (Q9I0X4), producing the β-ketoadipate enol-lactone as a point of metabolic convergence (Fig. 2). The first two enzymes of the second branch, *p*-hydroxybenzoate hydroxylase and protocatechuate 3,4-dioxygenase, which convert benzoate to 3-hydroxy and 3,4-dixydroxy derivatives were not found, while 3-carboxy-*cis, cis*-muconate cycloisomerase (Q9I6Q8) and *γ*-carboxymuconolactone decarboxylase (Q9I6Q6) which produce the common metabolite β-ketoadipate enol-lactone were identified. Finally, the β-ketoadipate enol-lactone was metabolized by β-ketoadipate enol-lactone hydrolase (Q9I6Q7), β-ketoadipyl-CoA thiolase (Q9I6R0) and acetyl-CoA acetyltransferase (Q9I2A8) to produce succinyl- CoA and acetyl -CoA, intermediates of the TCA cycle. Mandalakis et al., 2013 reported similar results for the degradation of benzoate by *P. putida* F1.

A few of these proteins were also detected in glucose grown bacteria (Table 3), suggesting that enzymes can be induced at low levels even in the absence of an inducer (Yun et al., 2011).

Table 3 Enzymes of β-ketoadipate pathway during the growth of *P. aeruginosa* san ai on sodium-benzoate and glucose. Number of identified peptides per protein from 3 biological replicates is shown. List of enzymes is based on KEGG-Id: pae00362.

Accession	Protein name	Gene	Peptides Glc	Peptides NaB	log2 FC	p-value
Q9I0W4	Toluate 1,2-dioxygenase alpha subunit	xylX	1/0/0	16/23/17		
Q9I0W5	Toluate 1,2-dioxygenase beta subunit	xylY	1/0/1	2/7/2		
Q9I0W7	Cis-1,2-dihydroxycyclohexa-3,4-diene carboxylate dehydrogenase	xylL	2/0/0	5/10/4		
Q9I0X5	Catechol 1,2-dioxygenase	catA	0/1/1	7/12/8		
Q9I0X3	Muconate cycloisomerase I	catB	0/0/0	11/10/9		
Q9I0X4	Muconolactone Delta-isomerase	catC	0/0/0	2/5/2		
Q9I6Q7	Beta-ketoadipate enol-lactone hydrolase	pcaD	0/0/0	3/5/3		
G3XD40	Probable acyl-CoA thiolase	PA3925	0/1/0	3/0/4		
Q9HZJ3	3-ketoacyl-CoA thiolase	fadA	3/3/3	5/4/5	0.7	3.32e-02
Q9I6R0	Beta-ketoadipyl-CoA thiolase	pcaF	2/0/2	13/22/17		
Q9I6Q8	3-carboxy-cis, cis-muconate cycloisomerase	pcaB	0/0/0	2/7/3		
Q9I6Q6	Gamma-carboxymuconolactone decarboxylase	pcaC	0/0/0	0/4/0		
Q9HZJ2	Fatty acid oxidation complex subunit alpha	fadB	16/16/17	13/12/16	0.18	1.69e-01
Q9I671	Glutaryl-CoA dehydrogenase	gcdH	5/4/2	3/5/2	-0,35	6.76e-02
Q9I002	Probable enoyl-CoA hydratase/isomerase	PA2841	3/1/1	3/4/4	0,27	7.13e-01

Q9I5I4	Probable enoyl-CoA hydratase/isomerase	PA0745	14/12/14	13/9/13	-0,43	1.80e-01
Q9I2Y9	Probable enoyl-CoA hydratase/isomerase	PA1748	4/5/4	7/3/8	-0.22	5.31e-01
Q9I0T1	Probable acyl-CoA thiolase	PA2553	11/18/19	23/15/26	1.38	2.28e-01
Q9I2A8	Acetyl-CoA acetyltransferase	atoB	18/18/19	20/13/19	0.93	1.53e-01

The results show that the majority of benzoate degradation pathway proteins are up regulated in the presence of sodium-benzoate. In sodium benzoate- grown cells the complete list of proteins involved in the *ortho*-degradation pathway of catechol (Fig. 3) was identified, while *meta*-cleavage pathway enzymes have not been detected. In accordance with our results, activities of the C120 and C230 catechol dioxygenases in cells grown on NaB, were probed, and a significantly higher activity of C120 than C230 (0.2 mU/mg and 0.001 mU/mg, respectively) was found, clearly indicating that benzoate was exclusively metabolized by the *ortho*- cleavage pathway. Besides, enzymatic tests demonstrated activity of hydroxylase (0.09 mU/mg) indicating ring activation, as an initial reaction of NaB degradation. These results are in correlation with our previous research data (Medić et al., 2019; 2020).

3.6.2. Similarity between glucose- and benzoate- grown P. aeruginosa san ai

The citric acid cycle (TCA) is the central metabolic hub of the cell and an important source of precursors for other biomolecules. Both of the examined pathways, the ED and the β-ketoadipate, add, in a controlled manner, their end products to the TCA. It is therefore not surprising that all enzymes of the TCA cycle coded by 28 genes in addition to the key enzymes of the glyoxylate shunt (malate synthase - Q9I636 and isocitrate lyase - Q9I0K4) and pyruvate shunt (malic enzyme- Q9HUD3) were detected in both of NaB and glucose grown cultures (Table 4).

Although the glyoxylate shunt, as an anaplerotic pathway, typically is not required in glucose-grown cells, enzymes isocitrate liase and malate synthase were nevertheless found in both cultures of *P. aeruginosa* san ai, grown in either of glucose or benzoate (Fig. 2, Table 4). Accordingly, study of metabolic pathway flux showed that at the level of isocitrate, approximately 20% of carbon was channeled into the shunt (Berger et al., 2014). The same

study indicated that the TCA cycle was continuously depleted by the anabolic requirement for its intermediate oxaloacetate (17%) suggesting that the anaplerotic route serves to replenish the TCA cycle.

Regarding pyruvate, several enzymes were identified: phosphoenolpyruvate carboxykinase (PEPCK) which catalyzes the conversion of oxaloacetate (OAA) to phosphoenolpyruvate (PEP) through direct phosphoryl transfer between the nucleoside triphosphate and OAA; oxaloacetate decarboxylase which catalyzes the decarboxylation of oxaloacetate into pyruvate and malic enzyme which catalyzes the conversion of malate into pyruvate; and NADPH, powering the pyruvate shunt, which returns carbon to the glycolytic pools (Fig. 2, Table 4). Pyruvate can be transformed by pyruvate dehydrogenase (PDH) complex, that catalyzes the overall conversion of pyruvate to acetyl-CoA and CO_2, and by phosphoenolpyruvate synthase which catalyzes the phosphorylation of pyruvate to phosphoenolpyruvate in the pathway gluconeogenesis whose enzymes were found to be similarly expressed (Table S3).

Table 4 Identified proteins of TCA cycle, glyoxylate and pyruvate shunt during the growth of *P. aeruginosa* san ai on sodium-benzoate and glucose (according to KEGG-Id: pae00020).

Accession	Protein name	Gene	Peptides Glc	Peptides NaB	log2 FC	p-value
Q9I2V5	Aconitate hydratase B	acnB	32/27/27	29/22/29	-0.37	2.05e-01
Q9I3F5	Aconitate hydratase A	acnA	14/13/12	10/15/6	-0.98	3.29e-03
Q9I0K4	Isocitrate lyase	PA2634	12/12/12	15/16/16	0.18	4.24e-01
Q9I636	Malate synthase G	glcB	8/5/8	4/13/4	-0.22	5.03e-01
Q9I0L5	Isocitrate dehydrogenase [NADP]	icd	33/30/34	27/33/31	-0.14	6.01e-01
Q9I0L4	Isocitrate dehydrogenase [NADP]	idh	6/11/11	24/22/25	2.86	4.44e-02
Q9I3D3	Oxoglutarate dehydrogenase (succinyl-transferring)	sucA	13/14/14	29/20/29	1.66	4.29e-02
Q51567	Succinate--CoA ligase [ADP-	sucD	29/29/28	25/23/28	-0.09	4.61e-01

	forming] subunit alpha					
P53593	Succinate--CoA ligase [ADP-forming] subunit beta	sucC	23/19/20	21/25/20	0.03	9.25e-01
Q9I3D5	Succinate dehydrogenase flavoprotein subunit	sdhA	17/20/19	31/26/31	1.81	6.42e-02
Q9I3D4	Succinate dehydrogenase (B subunit)	sdhB	10/9/9	13/8/13	0.63	1.74e-01
Q9HW68	Fumarate hydratase class I	PA4333	0/1/1	2/0/2		
Q9I587	Fumarate hydratase class II 1	fumC1	1/0/0	1/3/2		
Q51404	Fumarate hydratase class II 2	fumC2	7/7/5	8/8/10	0.38	2.09e-01
Q9HVF1	Probable malate:quinone oxidoreductase 2	mqo2	4/3/4	3/2/3	-1,19	3.34e-03
Q9HUD3	Malic enzyme	PA5046	35/28/32	37/27/36	-0.22	3.40e-01
P14165	Citrate synthase	gltA	5/6/6	16/16/14	1.52	1.15e-02
Q59637	Pyruvate dehydrogenase E1 component	aceE	20/21/21	19/24/20	0.06	6.75e-01
Q9I3D1	Dihydrolipoyl dehydrogenase	lpdG	28/31/29	31/20/29	-0.48	2.99e-01
Q9I1L9	Dihydrolipoyl dehydrogenase	lpdV	19/20/21	19/15/17	-1.69	1.45e-02
Q9HTZ7	Phosphoenolpyruvate carboxykinase (ATP)	pckA	23/20/21	21/18/23	0.35	3.78e-01
Q9HTD1	Probable transcarboxylase subunit	PA5435	14/14/13	18/19/17	0.45	4.02e-01
Q9I3D2	Dihydrolipoyllysine-residue succinyltransferase component of 2-oxoglutarate dehydrogenase complex	sucB	10/12/12	17/17/17	0.1	8.60e-01
Q59637	Pyruvate dehydrogenase E1 component	aceE	20/21/21	19/24/20	0,06	6.75e-01
Q59638	Dihydrolipoyllysine-residue acetyltransferase component of pyruvate dehydrogenase complex	aceF	11/14/13	13/8/12	-0.14	6.68e-01
Q9HTD0	Biotin carboxylase	PA5436	2/4/4	4/8/5	0.14	6.45e-01

Q9HVF1	Probable malate:quinone oxidoreductase 2	mqo2	4/3/4	3/2/3	-1.19	3.34e-03

Based on the number of identified peptides, there were no significant differences between growth of *P. aeruginosa* san ai on glucose and sodium-benzoate (Table 4). As a measure of intensive growth, a large number of ribosomal proteins (52), (Table S4), and amino acids biosynthetic proteins (85), (Table S5), were identified in both cultures indicating similar growth rates in both substrates.

Stress proteins. It is expected that *Pseudomonas* exposed to aromatic compounds exhibit a complex response that comprises three major programs: triggering the compound-specific metabolic pathways integrated within the global metabolism; stress-response adaptation to sub-optimal growth conditions; and a social program that implies cell motility, chemotaxis, quorum sensing, and biofilm formation (Nogales et al., 2017). We have considered and proven an unambiguous change in the compound-specific metabolic pathways- glucose triggered the ED pathway, while NaB induced the KA pathway. Surprisingly, stress proteins such as: catalase, superoxide dismutase, alkyl hydroperoxide reductase, thioredoxin reductase, thioredoxin peroxidase, thiol peroxidase, and almost all of enzymes of glutathione metabolism appeared in both cultures, demonstrating similar growth conditions that equally disturb redox homeostasis (Table S6). The only difference is thiol:disulfide interchange protein DsbC which is down regulated in benzoate- grown culture. The triggered pathways- the ED and the KA- efficiently regulate redox status providing a high tolerance to oxidative stress. Contrary to our results, some authors found significant differences in stress proteins between cells grown on gluconeogenic substrates (succinate, benzoate) (Mandalakis et al., 2013). Cao and Loh (2008) suggested that aromatic compounds may cause the overexpression of stress proteins for the protection of cells against oxidative damage. On the other hand, this study demonstrates that chaperones GroS, SurA and DnaK, which promote the proper folding of proteins under stress conditions, were found in similar amounts in *P. aeruginosa* san ai cells grown on either glycolytic (glucose) or gluconeogenic (benzoate) substrates, implying common stress responses. In the glucose amended culture the ED mediates better cope than the EMP to oxidative stress as this pathway provides NADPH (Chavarria et al., 2013). In the NaB supplemented cultures, up regulation of several

dehydrogenases including NAD-specific glutamate dehydrogenase (Q9HZE0) with 2-fold the number of peptides in NaB cells, aldehyde dehydrogenases (Q9HUR4) with 3-fold the number of peptides in NaB cells, Q9HTP2, Q9HX05, might be a source of NADH which could improve cellular reducing power to overcome oxidative stress (Table S1; Dietrich et al., 2008). Besides, the common dehydrogenases make up almost 6% of total number of proteins, indicates that both cultures are equally successful in NADH production.

Iron homeostasis. Aromatic dioxygenases, toluate 1,2-dioxygenase/ benzoate 1,2-dioxygenase, contain 2Fe-2S clusters responsible for electron transfer. As iron is essential for cell homeostasis and degradation of aromatic rings by dioxygenases, its concentration is strictly regulated. As a control of iron availability, a storage protein bacterioferritin and proteins of siderophores biosynthesis were detected in both cultures. *P. aeruginosa* san ai synthesizes a highly iron-specific siderophore- pyoverdine, and pyochelin with a broad specificity. In this sense, proteins of pyoverdine biosynthetic process including PvdO, PvdN, and PvdQ, in addition to Fe(3+)-pyochelin receptor were found to be almost equally represented. It is worth mentioning that acyl-homoserine lactone acylase PvdQ functions as a quorum quencher enabling *P. aeruginosa* to modulate its own quorum-sensing potential (Table S7).

Sulfur and nitrogen assimilation. Sulfur supply is critical for amino acids synthesis and for function of dioxygenases. In MSM grown cells of *P. aeruginosa* san ai increasingly produced sulfate-binding protein and sulfide reductase according to assimilatory sulfate reduction map, (KEGG map M0017), (Table S8, S10), but no preferential expression of protein such as arylsulfatase in benzoate-grown cells was detected, although this enzyme was considered as vital for *P. putida* and its survival in the soil environment (Mandalakis et al., 2013). Our results are in agreement with the finding that inorganic sulfate reduced the expression of arylsulfatases (Kertesz, 2000).

Two routes for ammonia assimilation exist in *P. aeruginosa* san ai: NAD-specific glutamate dehydrogenase (Q9HZE0) that incorporates ammonia into glutamate, and glutamine synthetase (Q9HU65) which catalyzes the ATP-dependent incorporation of ammonia in glutamate to form glutamine (Table S5). In benzoate amended cultures, NAD-specific glutamate dehydrogenase is up regulated, while synthesis of glutamine synthetase is equally pronounced in both cultures (more than 35 identified peptides per protein Q9HU65).

DNA-binding transcriptional regulator of NtrC (Q9HU59) which controls ammonia uptake under nitrogen-limited conditions, in addition to nitrogen regulatory proteins (Q9HVV4 and Q9HTR6) were identified (Gyaneshwar et al., 2005).

Amino acids. Metabolism and transport of amino acids which was found to be very sensitive to changes in carbon source (Medić et al., 2019) did not show disturbance caused by glycolytic (glucose) or gluconeogenic (benzoate) substrates. In fact, an intensive anabolism of amino acids takes place on both substrates (Table S5). Besides, proteins of either permease or ATP- binding domains of ABC (ATP-binding cassette) transporters responsible for uptake of amino acids or dipeptides were found to be equally regulated in cells grown on both substrates, which testifies that the membrane activity is not dependent on the added C-source (Table S8). Interestingly, the glycine cleavage system, which is highly sensitive to alterations in the oxidation–reduction state of the respiratory chain works in both cultures equally (Table S5). In both cultures, catabolic ornithine carbamoyltransferase was detected, implicating enhanced catabolism of arginine by the arginine deiminase (ADI) pathway. The catabolic ornithine carbamoyltransferase catalyzes the phosphorolysis of citrulline, yielding ornithine and carbamoyl phosphate which serve to generate ATP from ADP. Nevertheless, the ornithine was decarboxylated by ornithine decarboxylase present in both cultures yielding putrescine which further produces spermidine. Putrescine-binding periplasmic protein SpuD, spermidine-binding periplasmic protein SpuE, arginine/ornithine binding protein AotJ and amino acid (Lysine/arginine/ ornithine/ histidine/ octopine) ABC transporter periplasmic binding protein (Table S5) imply an enhanced polyamine production. Both *de novo* polyamine synthesis accompanied with bacteria polyamine transport systems suggest a significant adaptive and/or survival properties of *P. aeruginosa* san ai, as they play a crucial role in outer membrane functions, in protecting cells from reactive oxygen species, acidic stress etc. (Shah and Swiatlo, 2008). All proteins known to be involved in the pathway L-phenylalanine degradation that synthesizes acetoacetate and fumarate from L-phenylalanine were found in both cultures almost equally, while aromatic-amino-acid aminotransferase responsible for L-phenylalanine and L-tyrosine biosynthesis was significantly upregulated in benzoate- grown culture pointing to a role of benzoate in aromatic amino acid synthesis.

Transporters and outer membrane proteins. A large number of different transporters were found in both cultures and it has been already discussed in certain sections (Table S8). The outer membrane OprF, OprG, OprE, porin B, porin D are represented in the

same quantities, with the exception of OprM, OpdT and OpdP found only in benzoate. The identification of OprM, the major efflux pump for *n*-hexane and *p*-xylene, and efflux pump membrane transporter for xenobiotic (Q9I0Y8), in benzoate cultures only (Table S9), indicate the active response of the cell toward exposure to aromatic hydrocarbons, as reported earlier (Medić et al., 2019).

Social program. Although changes of social program that implies cell motility, quorum sensing, and biofilm formation in cultures amened with aromatic compounds (Nogales et al., 2017) were expected, this study demonstrated significant similarity between protein abundance profiles of *P. aeruginosa* san ai cells grown on glycolytic (glucose) or gluconeogenic (benzoate) substrates in sense of social program (Table S2). Cell surface structures composed from proteins: PilH, PilJ, PilQ, FliL, B-type flagellin, which form pilli that regulate twitching motility and fagella responsible for microbial adhesion, were found in similar amounts. Preferential expression of several proteins involved in flagellar motility found in *P. putida* F1 grown on citrate was explained as a side effect driven by the moderate toxicity of benzoate (Mandalakis et al., 2013). Domínguez-Cuevas et al. (2006) also reported a repression of the motility/chemotaxis and pilus/flagellum-related genes in *P. putida* KT2440 exposed to toluene. It seems, however, that in case of *P. aeruginosa* san ai motility was not reduced implying nontoxic effects of benzoate; in other words, the use of this substrate does not cause major metabolic changes related to motility. Proteins of pilli and flagella, whose enzymes and regulators for biosynthesis are present in both cultures, are involved in the early stages of *P. aeruginosa* biofilm formation (Toutain et al., 2004), were not significantly changed by C source (Table S2). As the motion of the flagellar motor consumes a considerable amount of intracellular ATP, energy requirement of both cultures was found to be similar with respect to the electron transfer flavoprotein (ETFA/B) and the ATP synthase, accompanied with the dihydrolipoyl dehydrogenase component of the α-ketoacid dehydrogenases complex, α-ketoglutarate dehydrogenase and pyruvate dehydrogenase complexes, which produce NADH and provide electrons for the respiratory chain and consequently for ATP supply (Table S1).

4. Conclusions

P. aeruginosa san ai can cope with a broad range of environmental challenges, from high pH and heavy metals, to organic solvents and hydrocarbons, particularly aromatics. A

very high resistance to sodium benzoate of 18 mg/mL was determined, confirming another remarkable property of the extremophilic bacterium. The similar growth rate of *P. aeruginosa* san ai when cells used glucose or sodium benzoate, as the sole C- source in minimal mineral medium, implies that the two compounds are equally good carbon sources, and that benzoate, in concentrations found in the environment, has no toxic effect on the bacterium. In response to physiological conditions regarding carbon sources- glucose and sodium benzoate, induction of the Entner- Doudoroff and the β-ketoadipate pathways was investigated. Genome analysis of *P. aeruginosa* san ai indicated existence of all genes of the ED and the KA pathways, whereas enzymes of these pathways were identified in cells grown on particular C-source- glucose and benzoate, respectively, using functional proteomic approach. All metabolic intermediates of the KA pathway were confirmed by targeted metabolomic analysis in benzoate- grown cells. Functional analysis of exclusively identified proteins from *P. aeruginosa* san ai indicated a pronounced secondary metabolism of benzoate grown culture that implies amplified aromatic compound catabolism, while in glucose grown culture extracellular structures synthesis were found to be enhanced. Aside of unique proteins, more than 75% of proteins are common for both, glucose- and benzoate- amended culture. The products from both examined pathways, the ED and the KA, enter the TCA cycle, whose all enzymes, in addition to the key enzymes of the glyoxylate and pyruvate shunt were detected in both cultures, grown on benzoate and glucose. In both cultures, the electron transfer flavoprotein (ETFA/B) and the ATP synthase were equally identified, accompanied with certain dehydrogenases which produce NADH, and the ADI pathway, which provide electrons for the respiratory chain and consequently for ATP supply. It is intriguing that both triggered pathways, the ED and the KA, efficiently regulate redox status and equally mediate a high tolerance to oxidative stress. Significant similarity between cell motility and biofilm formation of *P. aeruginosa* san ai cells grown on glycolytic or gluconeogenic substrates in sense of equally efficient social program, was demonstrated as well.

Considering all the above similarities in metabolic responses as well as the unique, induced carbon catabolic pathways, *P. aeruginosa* san ai appears to exhibit exceptional resistance to benzoate with remarkable metabolic plasticity and potential to survive in a toxic environment by efficiently adapting its complex life machinery. This ability can offer wide range of application of this strain in environmental biotechnology.

Author contributions

Conceptualization; Supervision: I.K., Z.M., M.B.; Methodology: A.M., M.Lj., N.H., Y.R.; Software, Formal analysis: N.H., Y.R., A.M., Z.M.; Investigation: all authors; Resources: genome, metabolome study, enzyme assays, sample preparation of protein extracts: A.M., M.Lj., I.K., proteome study: N.H., Y.R., M.B., Z.M.; Writing - Review & Editing: A.M., N.H., Y.R., M.Lj. (writing), I.K., Z.M., M.B. (review & editing); Visualization: A.M., N.H., Y.R.; Project administration; Funding acquisition: A.M., I.K.

Acknowledgments

This work was supported by the Ministry of Education, Science and Technological Development of Republic of Serbia (Projects III 43004 and 176006). The authors would like to thank Dr Branka Lončarević for assistance with respiration experiments.

Declaration of Competing Interest

The authors report no declarations of interest.

References

Avramović, N., Nikolić-Mandić, S., Karadžić, I., 2013. Influence of rhamnolipids, produced by *Pseudomonas aeruginosa* NCAIM(P), B001380 on their Cr (VI) removal capacity in liquid medium. J. Serb. Chem. Soc. 78, 639-651.

Benedek, T., Szentgyörgyi, F., Szabó, I., Farkas, M., Duran, R., Kriszt, B., Táncsics, A., 2020. Aerobic and oxygen-limited naphthalene-amended enrichments induced the dominance of *Pseudomonas spp*. from a groundwater bacterial biofilm. Appl. Microbiol. Biotechnol. 104, 6023-6043.

Bradford, M.M., 1976. A rapid and sensitive method for the quantitation of microgram quantities of protein utilizing the principle of protein-dye binding. Anal. Biochem. 72, 248-254.

Cao, B., Loh, K.C., 2008. Catabolic pathways and cellular responses of *Pseudomonas putida* P8 during growth on benzoate with a proteomics approach. Biotechnol. Bioeng. 101 (6), 15.

Chae, H.J., Yoo, Y.J, 1997. Mathematical modelling and simulation of catechol production from benzoate using resting cells of *Pseudomonas putida*. Process Biochem. 32 (5), 423-432.

Chauhan, A., Jain, R. Biodegradation: gaining insight through proteomics. Biodegradation 2010;21(6):861-79. doi: 10.1007/s10532-010-9361-0.

Chavarria, M., Nikel, P.I., Perez-Pantoja, D., de Lorenzo, V., 2013. The Entner- Doudoroff pathway empowers *Pseudomonas putida* KT2440 with a high tolerance to oxidative stress. Environ. Microbiol. 15, 1772-1785.

Chen, I.A., Chu, K., Palaniappan, K., Pillay, M., Ratner, A., Huang, J., Huntemann, M., Varghese, N., White, J.R., Seshadri, R., Smirnova, T., Kirton, E., Jungbluth, S.P., Woyke, T., Eloe-Fadrosh, E.A., Ivanova, N.N., Kyrpides, N.C., 2019. IMG/M v.5.0: an integrated data management and comparative analysis system for microbial genomes and microbiomes. Nucleic Acids Res. 47, D666-D677.

Cox, J.; Mann, M., 2008. MaxQuant enables high peptide identification rates, individualized p.p.b.-range mass accuracies and proteome-wide protein quantification. Nat. Biotechnol. 26, 1367-1372.

Cox, J.; Neuhauser, N.; Michalski, A.; Scheltema, R.A.; Olsen, J.V.; Mann, M., 2011. Andromeda: a peptide search engine integrated into the MaxQuant environment. J. Proteome Res. 10, 1794-1805.

del Castillo, T., Ramos, J.L., Rodriguez-Herva JJ, Fuhrer, T., Sauer, U., Duque, E., 2007. Convergent peripheral pathways catalyze initial glucose catabolism in *Pseudomonas putida*: genomic and flux analysis. J. Bacteriol. 189, 5142-5152.

Dietrich, L.E., Teal, T.K., Price-Whelan, A., Newman, D.K., 2008. Redoxactive antibiotics control gene expression and community behavior in divergent bacteria. Science. 321, 1203-1206.

Dolan, S.K., Kohlstedt, M., Trigg, S., Vallejo Ramirez, P., Kaminski, C.F., Wittmann, C., Welch, M., 2020. Contextual flexibility in *Pseudomonas aeruginosa* central carbon metabolism during growth in single carbon sources. mBio. 11, e02684-19.

Domínguez-Cuevas, P., González-Pastor, J.E., Marqués, S., Ramos, J.L., de Lorenzo, V., 2006. Transcriptional tradeoff between metabolic and stress-response programs in *Pseudomonas putida* KT2440 cells exposed to toluene. J. Biol. Chem. 281, 11981-11991.

Fuhrer, T., Fischer, E., Sauer, U., 2005. Experimental identification and quantification of glucose metabolism in seven bacterial species. J. Bacteriol. 187, 1581-1590.

Ghosal, D., Ghosh, S., Dutta, T.K., Ahn, Y., 2016. Current state of knowledge in microbial degradation of polycyclic aromatic hydrocarbons (PAHs): A review. Front. Microbiol. 7, 1369.

Gorisch H., Jeoung, J.H., Ruckert, A., Kretzschmar, U., 2002. Malate:quinone oxidoreductase is essential for growth on ethanol or acetate in *Pseudomonas aeruginosa*. Microbiology. 148, 3839-3847.

Gouveia, D., Almunia, C., Cogne, Y., Pible, O., Degli-Esposti, D., Salvador, A., Cristobal, S., Sheehan, D., Chaumot, A., Geffard, O., Armengaud, J., 2019. Ecotoxicoproteomics: A decade of progress in our understanding of anthropogenic impact on the environment. J. Proteomics. 198, 66-77.

Harwood, C.S., Parales, R.E., 1996. The β-ketoadipate pathway and the biology of self-identity. Annu. Rev. Microbiol. 50, 553-590.

He, H., Zhu, W., Noor, I., Liu, J., Li, G., 2019. *Pseudomonas putida* WH-B3 degrades benzoic acid and alleviates its autotoxicity to peach (Prunus persica L. batsch) seedlings grown in replanted soil. Sci. Hortic. 255, 183-192.

Heyd, M., Kohnert, A., Tan, T.H., Nusser, M., Kirschhöfer, F., Brenner-Weiss, G., Franzreb, M., Berensmeier, S., 2008. Development and trends of biosurfactant analysis and purification using rhamnolipids as an example. Anal. Bioanal. Chem. 391, 1579-1590.

Huang, C., Xu, L., Sun, J., Zhang, Z., Fu, M., Teng, H., Yi, K., 2020. Allelochemical p-hydroxybenzoic acid inhibits root growth via regulating ROS accumulation in cucumber (Cucumis sativus L.). J. Integr. Agric. 19(2), 518-527.

Hugouvieux-Cotte-Pattat, N., Kohler, T., Rekik, M., Harayama, S., 1990. Growth-phase-dependent expression of the *Pseudomonas putida* TOL plasmid pWW0 catabolic genes. J. Bacteriol 172, 6651-6660.

Izrael-Živković, L., Rikalović, M., Gojgić-Cvijović, G., Kazazić, S., Vrvić, M., Brčeski, V., Lončarević, B., Gopčević, K., Karadžić, I., 2018. Cadmium specific proteomic responses of a highly resistant *Pseudomonas aeruginosa* san ai. RSC Adv. 8, 10549-10560.

Kanehisa, M., Goto, S.; 2000. KEGG: Kyoto Encyclopedia of Genes and Genomes. Nucleic Acids Res. 28, 27-30.

Katayama-Hirayama, K., Tobita, S., Hirayama, K., 1991a. Metabolic pathway of phenol in *Rhodotorula rubra*. J. Gen. App. Microbiol. 37, 379-388.

Katayama-Hirayama, K., Tobita, S., Hirayama, K., 1991b. Degradation of phenol by yeast *Rhodotorula rubra*, J. Gen. App. Microbiol. 37, 147-156.

Karadzic, I., Masui, A., Fujiwara, N., 2004. Purification and characterization of a protease from *Pseudomonas aeruginosa* growth in cutting oil. J. Biosci. Bioeng. 98, 145-152.

Karadžić, I., Masui, A., Izrael-Živković, L., Fujiwara, N., 2006. Purification and characterization of an alkaline lipase from *Pseudomonas aeruginosa* isolated from putrid mineral cutting oil as metal working fluid. J. Biosci. Bioeng. 102, 82-89.

Kertesz, M.A., 2000. Riding the sulfur cycle-metabolism of sulfonates and sulfate esters in gram-negative bacteria. FEMS Microbiol. Rev. 24, 135-175.

Kim, S.I., Kim, J.Y., Yun, S.H., Kim, J.H., Leem, S.H., Lee, C., 2004. Proteome analysis of *Pseudomonas sp* K82 biodegradation pathways. Proteomics. 4 (11), 3610-3621.

Kim, Y.H., Cho, K., Yun, S.H., Kim, J.Y., Kwon, K.H., Yoo, J.S., Kim, S.I., 2006. Analysis of aromatic catabolic pathways in *Pseudomonas putida* KT 2440 using a combined proteomic approach: 2-DE/MS and cleavable isotope-coded affinity tag analysis. Proteomics. 6(4), 1301-1318.

Kim, J., Park, W., 2014. Oxidative stress response in *Pseudomonas putida*. App. Microbiol. Biotechnol. 98, 6933-6946.

Li, Y., Ren, Y., Jiang, N., 2017. Analysis of draft genome sequence of *Pseudomonas* sp. QTF5 reveals its benzoic acid degradation ability and heavy metal tolerance. Biomed. Res. Int. 2017, 4565960.

Loh, K., Chua, S., 2002. Ortho pathway of benzoate degradation in *Pseudomonas putida*: induction of meta pathway at high substrate concentrations. Enzyme Microb. Technol. 30, 620-626.

Mandalakis, M., Panikov, N., Dai, S., Ray, S., Karger, B., 2013. Comparative proteomic analysis reveals mechanistic insights into *Pseudomonas putida* F1 growth on benzoate and citrate. AMB Express. 3, 64.

Medić, A., Stojanović, K., Izrael-Živković, L., Beškoski, V., Lončarević, B., Kazazić, S., Karadžić, I., 2019. A comprehensive study of conditions of the biodegradation of a plastic additive 2,6-di-tert-butylphenol and proteomic changes in the degrader *Pseudomonas aeruginosa* san ai. RSC Adv. 9, 23696.

Medić A, Lješević M, Inui H, Beškoski V, Kojić I, Stojanović, K., Karadžić, I., 2020. Efficient biodegradation of petroleum *n*-alkanes and polycyclic aromatic hydrocarbons by polyextremophilic *Pseudomonas aeruginosa* san ai with multidegradative capacity. RSC Adv. 10, 14060.

Nagaraj, N.; Kulak, N.A.; Cox, J.; Neuhauser, N.; Mayr, K.; Hoerning, O.; Vorm, O.; Mann, M., 2012. System-wide perturbation analysis with nearly complete coverage of the yeast proteome by single-shot ultra HPLC runs on a bench top Orbitrap. Mol. Cell. Proteomics. 11, M111.013722.

National committee for clinical laboratory standards, 1997. Methods for dilution antimicrobial susceptibility tests for bacteria that grow aerobically. Approved Standard M7- A4: Wayne PA.

Nogales, J., García, J.L., Díaz, E., 2017. Degradation of aromatic compounds in *Pseudomonas*: A systems biology view. Handbook of Hydrocarbon and Lipid Microbiology, Aerobic Utilization of Hydrocarbons, Oils, and Lipids, Rojo, F. (Ed.), Springer, Cham, pp. 1-49.

Opinion on benzoic acid and sodium benzoate, 2005. Scientific committee on consumer products, European commission health & consumer protection directorate-general, SCCP/0891/05.

Ornston, L. N., 1971. Regulation of catabolic pathways in *Pseudomonas*. Bacteriol. Rev. 35, 87-116.

Rikalović, M., Abdel-Mawgoud, A.M., Déziel, E., Gojgić-Cvijović, G., Nestorović, Z., Vrvić, M., Karadžić, I., 2013. Comparative analysis of rhamnolipids from novel environmental isolates of *Pseudomonas aeruginosa*. J. Surfact. Deterg. 16, 673-682.

Risha, Y., Minic, Z., Ghobadloo, S., Berezovski, V., 2020. The proteomic analysis of breast cell line exosomes reveals disease patterns and potential biomarkers. Sci. Rep. 10, 13572.

Rojo, F., 2010. Carbon catabolite repression in *Pseudomonas*: optimizing metabolic versatility and interactions with the environment. FEMS Microbiol. Rev. 34, 658-684.

Shah, P., Swiatlo, E., 2008. A multifaceted role for polyamines in bacterial pathogens. Mol. Microbil. 68: 4-16.

Stanojevic, D., Comic, Lj., Stefanovic, O., Solujic, S., 2009. Antimicrobial effects of sodium benzoate, sodium nitrite and potassium sorbate and their synergistic action in vitro. Bulg. J. Agric. Sci. 15(4), 308-312.

Toutain, C.M., Caiazza, N.C., O'Toole, G.A., 2004. Molecular basis of biofilm development by pseudomonads, Ghannoum, M., O'Toole, G.A. (Eds.), Microbial biofilms. ASM Press, Washington, DC, p. 43-63.

Tsirogianni, I., Aivaliotis, M., Karas, M., Tsiotis, G., 2004. Mass spectrometric mapping of the enzymes involved in the phenol degradation of an indigenous soil pseudomonad. Biochim. Biophys. Acta. 1700, 117-123.

Vandera, E., Samiotaki, M., Parapouli, M., Panayotou, G., Koukkou, A.I., 2015. Comparative proteomic analysis of *Arthrobacter phenanthrenivorans* Sphe3 on phenanthrene, phthalate and glucose. J. Proteom. 113, 73-89.

Varjani, S.J., Gnansounou, E., Pandey, A., 2017. Comprehensive review on toxicity of persistent organic pollutants from petroleum refinery waste and their degradation by microorganisms. Chemosphere. 188, 280-91.

Weimer, A., Kohlstedt, M., Volke, D., Nikel, P., Wittmann, C., 2020. Industrial biotechnology of *Pseudomonas putida*: advances and prospects, Appl. Microbiol. Biotechnol. 104, 7745-7766.

Xiang, W., Wei, X., Tang, H., Li, L., Huang, R., 2020. Complete genome sequence and biodegradation characteristics of benzoic acid-degrading bacterium *Pseudomonas* sp. SCB32. Biomed. Res. Int. 2020, 6146104.

Yun, S.H., Park, G.W., Kim, J.Y., Kwon, S.O., Choi, C.W., Leem, S.H., Kwon, K.H., Yoo, J.S., Lee, C., Kim, S., Kim, S.I., 2011. Proteomic characterization of the *Pseudomonas putida* KT2440 global response to a monocyclic aromatic compound by iTRAQ analysis and 1DE-MudPIT. J. Proteom. 74, 620-628.

Figure captions

Fig. 1. Growth and biodegradation of sodium-benzoate by *P. aeruginosa* san ai. a) Growth on increasing concentrations of NaB in LB medium. b) Intensity of cell growth on sodium-benzoate (3 mmol/L) and glucose (5 mmol/L) in MSM. c) Dynamics of sodium-benzoate (3 mM) degradation and cumulative CO_2 production during the growth of *P. aeruginosa* san ai on NaB (circle) and glucose (square) and d) O_2 consumption (controls were subtracted). Each data point represents the mean of three replicate samples. Some error bars are not visible because they are shorter than the symbol size.

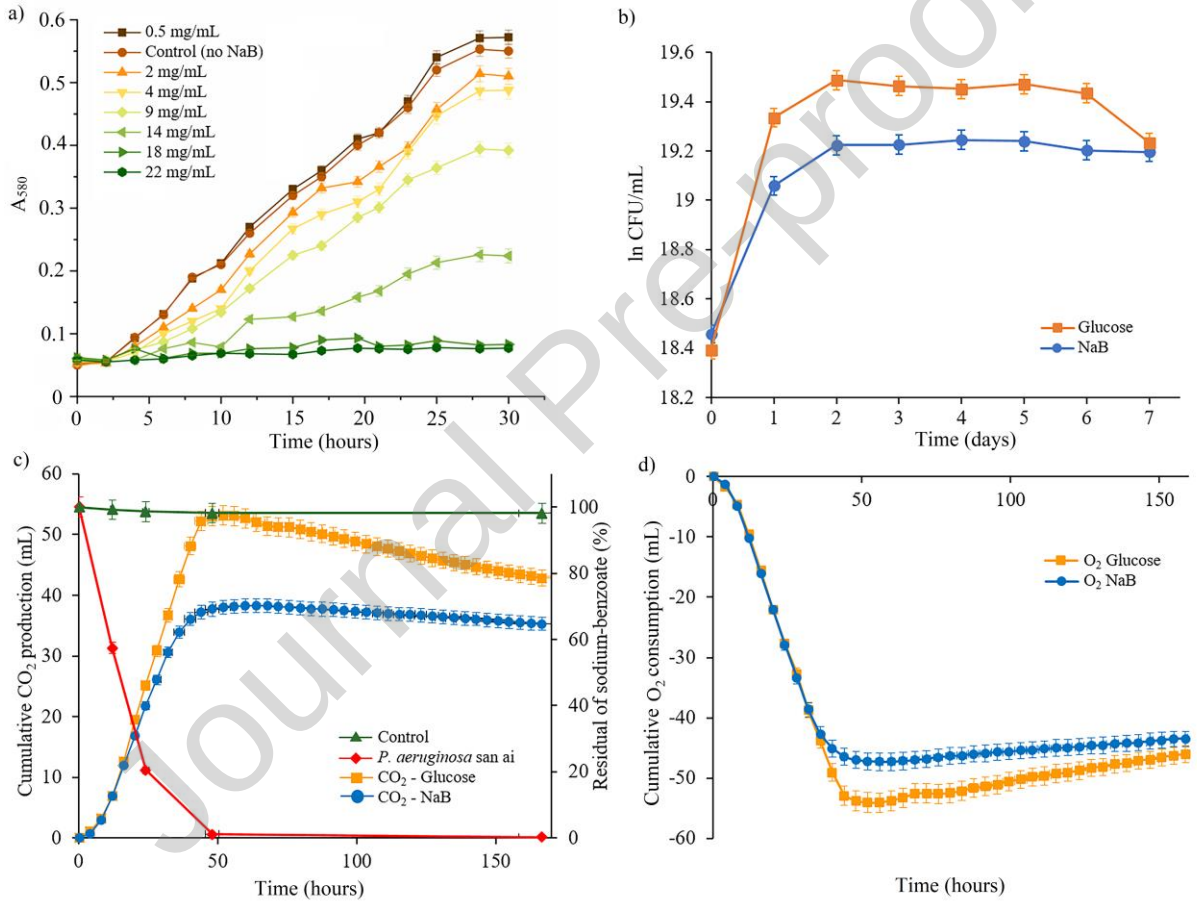

Fig. 2. Degradation pathway map of catabolism of benzoate and glucose and its connection with the tricarboxylic acid cycle in *P. aeruginosa* san ai. KA (β-ketoadipate pathway), TCA- tricarboxylic acid cycle, PYR- pyruvate, EDP- Entner-Doudoroff pathway, EMPP- Embden-Meyerhof- Parnas pathway.

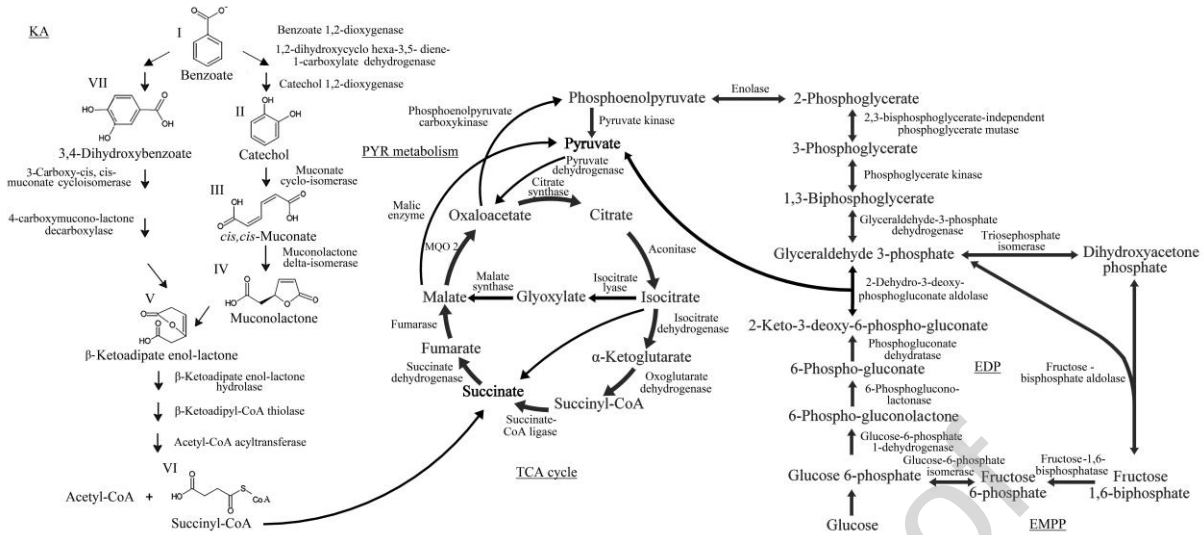

Fig. 3. A GCxGC-MS chromatogram of benzoate degradation after 24h. The metabolites of benzoate are marked from I-VII (see Table 1 for more details).

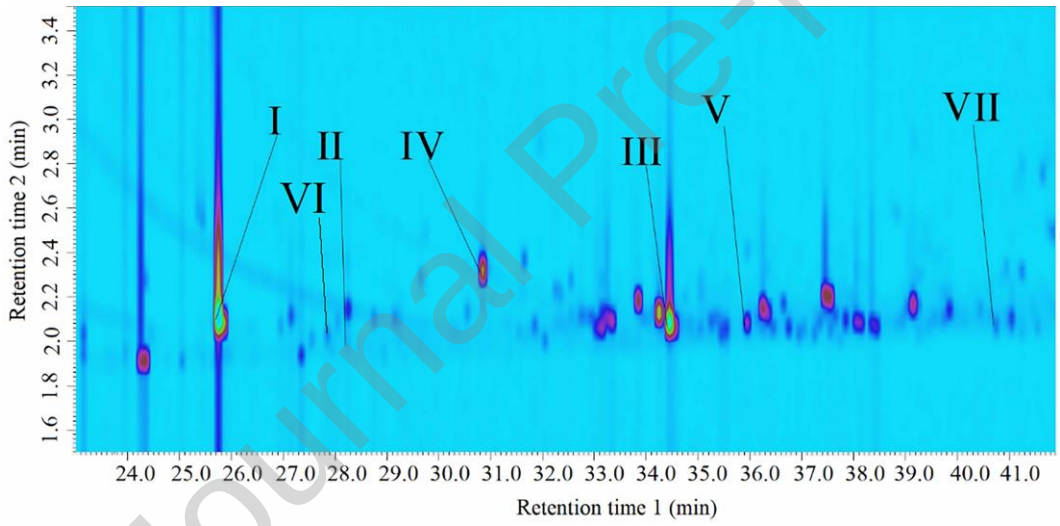

Fig. 4. Summary of protein identification in sodium benzoate- and glucose- grown culture. a) total number of identified proteins, b) functional classification of unique proteins from *P. aeruginosa* san ai grown in MSM supplemented with NaB and c) glucose. Metabolic categories, according to COG: A- RNA processing, C- energy production, E- amino acid metabolism, F- nucleotide metabolism, I- lipid metabolism, J- translation, G- carbohydrate metabolism, H- coenzyme metabolism, K- transcription, L- replication and repair, M- cell wall/ membrane/ envelope biogenesis, N- cell motility, O- PTM, chaperon function, P- inorganic ion transport, T- signal transduction mechanisms, U- secretion, V- defense

mechanism, Q- secondary metabolism, W- extracellular structures. Proteins with unknown S and general R function are not shown. COG categories-https://www.ncbi.nlm.nih.gov/COG/.

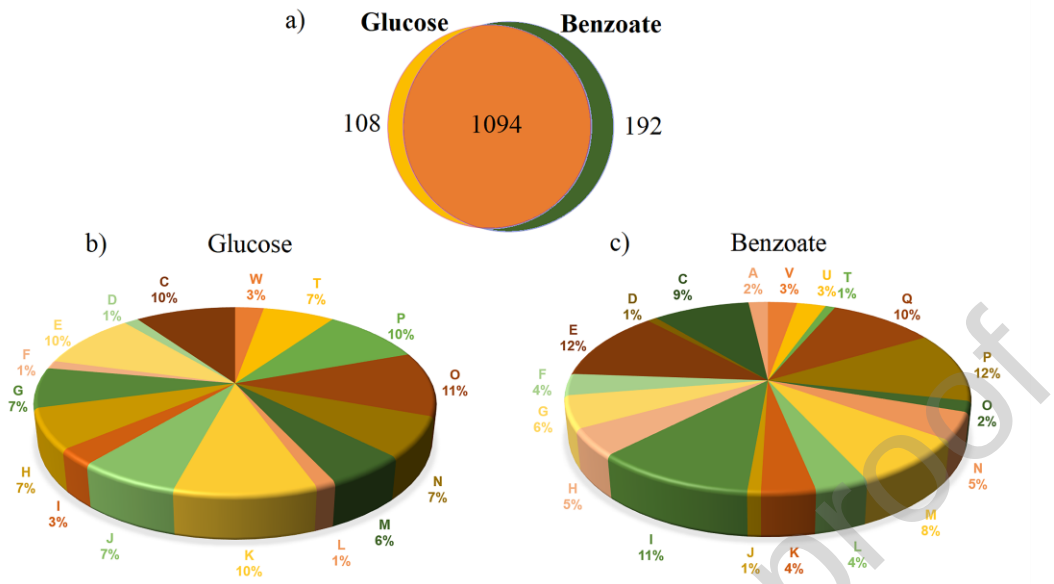

Graphical abstract

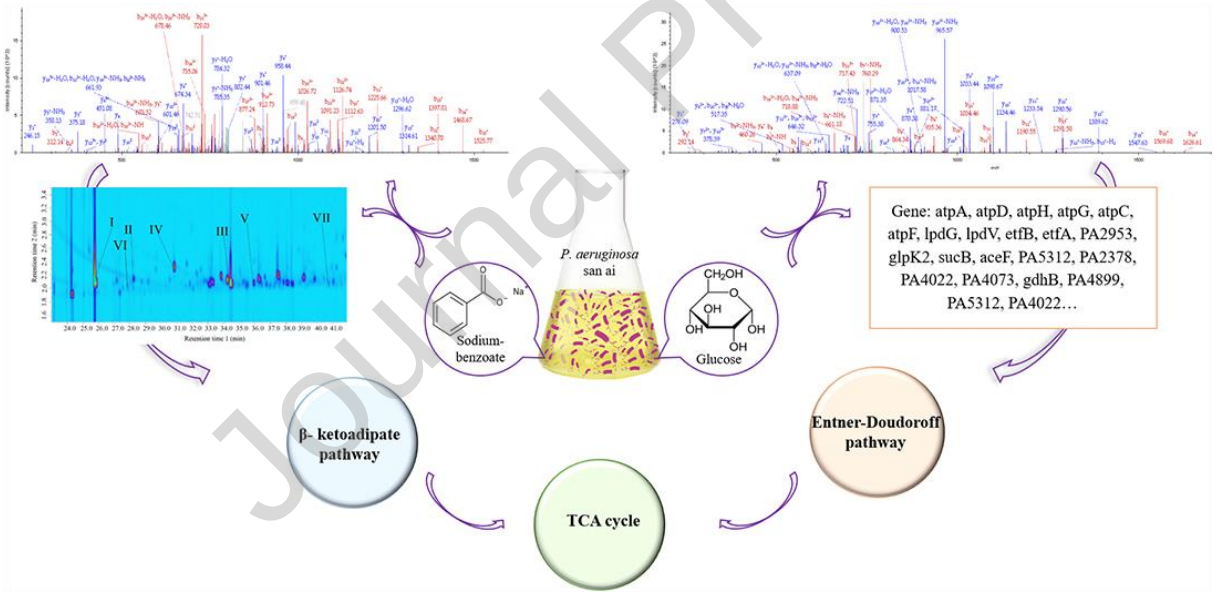

Declaration of interests

☒ The authors declare that they have no known competing financial interests or personal relationships that could have appeared to influence the work reported in this paper.

☐The authors declare the following financial interests/personal relationships which may be considered as potential competing interests: